

A Bioinformatic Approach Validated Utilizing Machine Learning Algorithms to Identify Relevant Biomarkers and Crucial Pathways in Gallbladder Cancer

Rabea Khatun^{1,2}, Wahia Tasnim², Maksuda Akter¹,
Md Manowarul Islam^{1*}, Dr. Md. Ashraf Uddin¹,
Dr. Md. Zulfiker Mahmud¹, Saurav Chandra Das^{1,2}

^{1*}Department of Computer Science and Engineering, Jagannath University, 9-10 Chittaranjan Ave, Dhaka, 1100, Bangladesh.

²Department of Computer Science and Engineering, Green University of Bangladesh, Purbachal American City, Kanchan, Rupganj, Narayanganj, 1461, Dhaka, Bangladesh.

*Corresponding author(s). E-mail(s): manowar@cse.jnu.ac.bd;
Contributing authors: rabeakhatun650@gmail.com;
wahiatasnim@gmail.com; maksudaoni6@gmail.com;
ashraf@cse.jnu.ac.bd; zulfiker@cse.jnu.ac.bd;
sauravchandradas@gmail.com;

Abstract

Gallbladder cancer (GBC) is the most frequent cause of disease among biliary tract neoplasms. Identifying the molecular mechanisms and biomarkers linked to GBC progression has been a significant challenge in scientific research. Few recent studies have explored the roles of biomarkers in GBC. Our study aimed to identify biomarkers in GBC using machine learning (ML) and bioinformatics techniques. We compared GBC tumor samples with normal samples to identify differentially expressed genes (DEGs) from two microarray datasets (GSE100363, GSE139682) obtained from the NCBI GEO database. A total of 146 DEGs were found, with 39 up-regulated and 107 down-regulated genes. Functional enrichment analysis of these DEGs was performed using Gene Ontology (GO) terms and REACTOME pathways through DAVID. The protein-protein interaction network was constructed using the STRING database. To identify hub genes, we

applied three ranking algorithms: Degree, MNC, and Closeness Centrality. The intersection of hub genes from these algorithms yielded 11 hub genes. Simultaneously, two feature selection methods (Pearson correlation and recursive feature elimination) were used to identify significant gene subsets. We then developed ML models using SVM and RF on the GSE100363 dataset, with validation on GSE139682, to determine the gene subset that best distinguishes GBC samples. The hub genes outperformed the other gene subsets. Finally, NTRK2, COL14A1, SCN4B, ATP1A2, SLC17A7, SLIT3, COL7A1, CLDN4, CLEC3B, ADCYAP1R1, and MFAP4 were identified as crucial genes, with SLIT3, COL7A1, and CLDN4 being strongly linked to GBC development and prediction.

Keywords: Gall bladder Cancer, Bioinformatics, Machine learning, HUB genes, PPI network, Differential gene expression

1 Introduction

The most prevalent form of Biliary Tract Cancer (BTC), Gallbladder Cancer (GBC) has an unfavourable outcome and a high death rate [1][2][3][4]. With an average survival of less than six months as well as a total five-year survival rate of under five percent, this malignancy is an extremely deadly illness. Since this cancer spreads quietly when a late diagnosis is made, early detection is crucial. With an ordinary cholecystectomy in suspicious gallbladder stone illness, 0.5–1.5% of patients were found with gallbladder cancer [5]. The eighth American Joint Committee on Cancer (AJCC) guideline [6] states that the most effective possible treatment for GBC at its infancy is surgical resection; for GBC at a later stage, chemotherapy, radiation therapy, immunotherapy, and targeted therapy are advised. The extremely aggressive and metastatic features of advanced GBC, such as local development of tumours, hepatic invasion, and lymph node metastases, result in minimal reaction to treatment and an unfavourable outlook for victims [7] [8]. While the complicated procedure and the molecular mechanism of GBC are ambiguous, numerous investigations have stated the essential function of numerous biological processes in cancer spread and invasion, including immune evasion [9], epithelial-mesenchymal transition (EMT) [10] [11], and cancer stem cells [12]. In order to enhance the prognosis for GBC patients, it is imperative to investigate the novel biomarkers linked to invasion and spreading.

An emerging method in studies on cancer for discovering pathways and genes as potential prognostic and diagnostic biomarkers is transcriptome analysis of high-throughput sequencing, such as microarrays and RNA sequencing [13] [14]. Additionally, bioinformatics are currently employed to uncover biomarkers linked to certain diseases. An advancement in the better prevention and treatment of GBC could be achieved by these biomarkers [15]. Relevant gene biomarkers for GBC are currently being identified by bioinformatic analysis of gene expression data; yet, the behaviour of the findings of bioinformatics is inconsistent. The predictive importance of several DEGs in GBC has been shown by current research. But the outcomes of such research have been inconsistent, maybe because various statistical techniques were employed. Furthermore, there is still a shortage of examination of the predictive significance of

the DEGs utilising machine learning technologies in GBC. Moreover, the enrichment pathways, Gene Ontology (GO) functions, and interaction network of DEGs are still unclear. A combination of bioinformatic methodologies and machine learning techniques can yield trustworthy outcomes and improve the GBC biomarker training and verification process[16].

This study is significant since it utilised bioinformatics and machine learning to analyse crucial genes for GBC and validate their diagnostic usefulness. This study is started by collecting 2 GBC-associated microarray datasets from gene expression omnibus database. We employed bioinformatics to identify key DEGs in GBC from microarray datasets. DEGs are offered for further functional investigation and protein-protein interaction analysis. We also identified top 15 hub genes using degree, maximum neighborhood component (MNC), and closeness methods. The intersection of the 11 hub genes identified by the three methods was thought to hold the "real" hub genes. Additionally, significant genes were found using feature selection methods such as pearson correlation and the recursive feature elimination technique. Afterwards, the 11 real hub genes and significant genes, identified by feature selection method, are trained on GSE 100363 dataset to develop machine learning model using support vector machine (SVM) and random forest (RF) algorithm. Finally, the model was tested using independent GSE 139682 dataset to validate the biomarkers. In addition, the 11 real hub genes were validated using GEPIA database. Step by step process of this study is demonstrated in Figure 1.

1.1 Research Gap

Despite significant advancements in understanding gallbladder cancer (GBC), several gaps persist in previous research. While numerous studies have highlighted the essential roles of various biological processes in cancer spread and invasion, the detailed molecular mechanisms of GBC remain elusive. Specifically, prior research has identified key biological processes such as immune evasion [9], epithelial-mesenchymal transition (EMT) [10] [11], and cancer stem cells as critical in GBC progression, yet the precise pathways and interactions governing these processes are not fully understood. Current approaches have largely relied on traditional bioinformatics and high-throughput sequencing methods, such as microarrays and RNA sequencing, to identify potential diagnostic and prognostic biomarkers. There has been limited application of machine learning technologies to examine the predictive significance of differentially expressed genes (DEGs) in GBC. This lack of integration of machine learning methods may hinder the ability to achieve more reliable and reproducible outcomes. Moreover, while gene expression data have been extensively analyzed to identify relevant biomarkers for GBC, there remains a significant gap in understanding the enrichment pathways, Gene Ontology (GO) functions, and interaction networks of these DEGs. Previous studies have not thoroughly investigated these aspects, which are crucial for elucidating the underlying biological mechanisms and for developing effective therapeutic strategies. Addressing these gaps is essential for advancing the diagnosis, treatment, and prognosis of GBC, and for providing a more comprehensive understanding of this aggressive cancer.

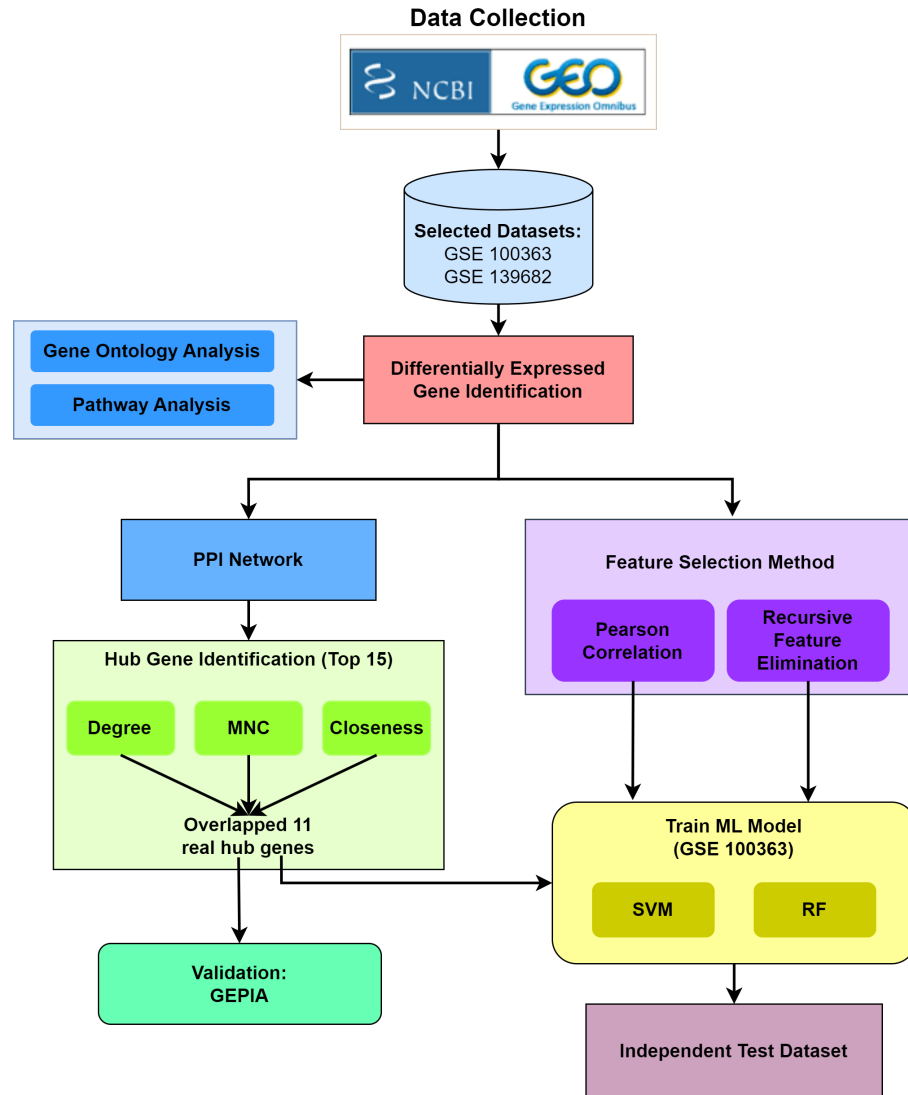


Fig. 1: Flow diagram of proposed methodology: Firstly, two microarray datasets (GSE100363, GSE139682) were downloaded from GEO. Secondly, differentially expressed genes (DEGs) were identified from those datasets. Next, the Gene Ontology analysis and Pathway analysis was performed with the identified DEGs to screen significant GO terms and pathways. After that, the protein-protein interaction (PPI) network was constructed. Subsequently, three ranking algorithms (Degree, MNC, Closeness Centrality) was employed to identify top 15 hub genes which, surprisingly, provided overlapped 11 real hub genes. In parallel, two feature selection methods (pearson correlation and recursive feature elimination) was employed to further identify significant gene subsets. Afterwards, the hub genes and significant genes subset were trained on GSE 100363 dataset to develop machine learning model using SVM and RF algorithm. Finally, the model was tested using independent GSE 139682 dataset to validate the biomarkers. Additionally, the real hub genes were validated using GEPIA database.

1.2 Research Question

This study aims to identify and validate key biomarkers for gallbladder cancer (GBC) using a combination of bioinformatics and machine learning techniques. Specifically, it seeks to answer the following questions:

- How can bioinformatics and machine learning approaches be used to identify biomarkers for gallbladder cancer (GBC) and which method produces optimal biomarkers for gallbladder cancer (GBC)?
- Which differentially expressed genes (DEGs) are significant in distinguishing between GBC and healthy samples?
- How can machine learning models be validated to accurately classify GBC samples based on these DEGs?
- What are the potential diagnostic and prognostic values of the identified hub genes and DEGs in GBC?

These questions arise from the need to enhance the precision of diagnostic and prognostic biomarkers, which are crucial for the effective treatment and management of GBC. Additionally, these questions aim to bridge the gap between traditional clinical methods and modern computational techniques by leveraging the power of high-throughput gene expression data and advanced algorithms. Specifically, the study seeks to identify differentially expressed genes (DEGs) that can serve as reliable biomarkers for GBC, develop predictive models using these biomarkers, and validate the effectiveness of these models in distinguishing between healthy and cancerous samples.

2 Methods

2.1 Data Collection

Gene Expression Omnibus (GEO, <https://www.ncbi.nlm.nih.gov/geo/>) of National Center for Biotechnology Information (NCBI) [17] is an accessible, high-throughput genome database that includes microarrays, chips, and gene expression data. The database, established in 2000, includes high-throughput gene expression data from research organisations worldwide. The repository provides access to published articles and associated gene expression detection data [18]. To find gene expression datasets for Gallbladder Cancer in the GEO database, we employed the search phrase "Gallbladder Cancer AND Homo sapiens" refined by "expression profiling by array". We obtained a pair of datasets (GSE100363 and GSE139682) produced on the GPL20795 platform, HiSeq X Ten (Homo sapiens), containing gene expression data for those suffering from gall bladder tumours and normal people. The GSE100363 series comprises 8 samples: 4 gallbladder tumours and 4 normal samples. The GSE139682 series comprises 20 samples: 10 gallbladder tumors and 10 normal samples. Figure 2 shows the distribution of tumour and normal sample counts across selected datasets..



Fig. 2: Distribution of number of samples of both tumor and normal among selected datasets. The GSE139682 series comprises 20 samples: 10 gallbladder tumors and 10 normal samples. The GSE100363 series comprises 8 samples: 4 gallbladder tumours and 4 normal samples.

2.2 DEG Identification

Differentially expressed genes (DEGs) refer to genes whose expression levels change significantly between different experimental conditions, such as different tissues, developmental stages, or disease states. Upregulated genes show higher expression levels in one condition compared to another. Conversely, downregulated genes exhibit lower expression levels in one condition compared to another. The upregulation of genes can indicate activation of specific biological processes, response to environmental stimuli, or involvement in disease pathways. On the other hand, the downregulation of genes may indicate suppression of certain biological processes, adaptation to environmental changes, or inhibition of disease pathways.

GEO2R (<http://www.ncbi.nlm.nih.gov/geo/geo2r>), a data analysis programme included within the GEO database, allows for visual statistical analysis of gene expression profiles. It examines multiple GEO series datasets to discover DEGs under experimental settings [19]. We utilised GEO2R to identify DEGs in both GBC tumour and normal samples. Utilising the GEO database, we acquired the gene $\log_2\text{foldchange}(\log_2FC)$ value. The ratio of the gene expression values for cancer and normal is expressed as a fold change of the gene. The upregulated and downregulated genes were determined by the positive and negative values of the \log_2FC values. Adjusted $P - \text{value} < 0.05$ and $|\log_2\text{foldchange}(\log_2FC)| > 1$ for overexpression along with $|\log_2\text{foldchange}(\log_2FC)| < -1$ for downexpression are employed to determine the statistically significant effect of genes. DEGs were visualized using a volcano map. Venn diagrams were created using the Venny online tool (<https://bioinfogp.cnb.csic.es/tools/venny/>) [20].

2.3 Gene Ontology and Pathway Enrichment Analysis of DEGs

Gene Ontology (GO) study yields broad biological research results for a particular gene or gene set by utilising the concepts of molecular functions (MFs), biological processes (BPs), and cellular components (CCs). The study of GO has become an essential component of investigations connected to system biology in recent times. Pathway enrichment analysis is another tool that helps investigate the biological relationships between gene sets derived from extensive genome-scale investigation [21]. In this work, the Gene Ontology database [22] was utilised to investigate the GO terms related with DEGs, and the REACTOME [23] databases were utilised to do pathway analysis. An online biological information directory called the Database for Annotation, Visualisation, and Integrated Discovery (DAVID, <http://david.abcc.ncifcrf.gov/>) combines biological data and analysis tools to offer a complete collection of annotation information for functional genes and proteins [24]. It offers a way for users to extract biological data. The DAVID online database was used to do biological studies and examine how DEGs work [22].

2.4 Protein–Protein Interaction (PPI) network construction

A public database called the Search Tool for the Retrieval of Interacting Genes/Proteins (STRING; <http://string-db.org>) is employed to anticipate the PPI networks[25]. Data on over 5000 species, 20 million proteins, and 3 billion interactions can be found in the STRING database. Such protein interactions encompass both co-expression correlations and direct physical interactions. To gain more knowledge of the intricate regulatory networks seen in organisms, known protein-protein connections can be discovered using the STRING database. According to earlier research, examining the functional relationships between proteins can reveal fresh information on the origin or progression of disorders[26]. Applying the STRING database, the PPI network of DEGs was created for this study.

2.5 Hub gene Identification

Hub genes are often utilised to focus on the subset of DEGs that would most effectively separate the ill samples from the control group. In turn, we visualised the constructed PPI network using the Cytoscape software [27] (<https://cytoscape.org/>), and we used the Cytoscape CytoHubba plugin to identify the hub genes in the PPI network using a variety of ranking techniques.

Various methods for node ranking, including local and global approaches, are offered by CytoHubba [28]. The global approach looks at the node’s interaction with the entire network, whereas the local ranking technique looks at the node’s interaction with its immediate peers. The hub genes were identified using three ranking algorithms: a global ranking method (Closeness Centrality), a pair of local ranking algorithms (Degree and Maximum Neighbourhood Component (MNC)). The quantity of nodes that surround a node v is its degree. Maximum connected component (MNC) is the size of the neighbourhood $N(v)$, which is the set of nodes that are next to v but do not contain v . Last but not least, closeness centrality, which is determined by averaging the length of the shortest path connecting a node to every other node in

the network, shows how close a node is to every other node in the network. In order to create machine learning models, we finally determined the top 15 genes from each ranking approach.

2.6 Identification of significant DEGs using feature selection methods

We used feature selection techniques, such as Pearson Correlation and Recursive Feature Elimination (RFE), which select the best features in high-dimensional data, to further find the important DEGs that best distinguish the diseased samples from the healthy controls. In a nutshell, RFE ranks the features according to their significance and returns the top-n features after eliminating the less significant ones, where n is the number of features that the user entered. In order to utilise it, the *estimator* parameter needs to be initialised by indicating the algorithm to be used and the *n_features_to_select* parameter by indicating the number of features to be selected. Following configuration, the model must be fitted to a training dataset using the *fit()* method in order to select the features. In our research, we supplied the sample matrix containing all of the features (146 DEGs) into the RFE model, setting *n_features_to_select* to 20 and using the SVM method as a *estimator*. Furthermore, Pearson correlation demonstrates the linear relationship between two variables. Strongly correlated features have a more linear dependence and so have a similar effect on the dependent variable. Two qualities may be eliminated if there is a substantial correlation between them. In our research, we entered the sample matrix including all 146 DEGs of features into a Pearson correlation model, compared the feature correlations, and removed one of the two features with a correlation higher than 0.9.

2.7 Developing ML models on GSE100363 dataset

For distinction among GBC tumours and healthy samples, we created two machine learning models i.e., Random Forest (RF) and Support Vector Machine (SVM) classification models. The applications of SVM, a supervised learning method, is in regression and classification. For classification purposes, the SVM generates hyperplanes that maximise the separation between classes. On the other hand, an ensemble classifier called Random Forest [29] [30] consists of many decision trees and produces a class that is the mode of the output of each tree individually. In every classification tree, a certain amount of votes are assigned to each class. Out of all the trees, the algorithm chooses the category with the highest number of votes.

Moreover, we developed a space of searches for parameter optimisation for each machine learning model in order to determine the optimal set of attributes. As a result, for hyperparameter optimisation in RF and SVM, we employed a grid search technique after randomised search. Regarding the randomised search, we generated a grid of hyperparameters, and we used random hyperparameter combinations to train and test our models. Subsequently, the optimal parameter combinations are determined by identifying the best parameters using randomised search. Table 1 summarizes the

tested parameters and selected parameters (highlighted in bold). We employed 4-fold-cross-validation (CV) to assess such models. The StratifiedKfold method is used to divide the data into four segments, assuring that each subgroup has an equal proportion of positive and negative observations. Choosing one of the subsets for testing and using all the other subsets for training allows the process to be performed four times. We computed the accuracy score for every fold and utilised that result for calculating the mean accuracy.

Model	Hyperparameters	Search Space
SVM	C Kernel Gamma	[0.1 , 1, 10, 100] [' linear ', 'rbf', 'poly'] [' scale ', 'auto', 0.1, 1]
RF	'n_estimators' 'max_depth' 'min_samples_split' 'min_samples_leaf'	[50 , 100 , 200] [None , 10, 20, 30] [2 , 5, 10] [1 , 2, 4]

Table 1: Search space parameters for RF and SVM model optimisation. The best parameter values are highlighted in bold.

2.8 Evaluation Tools

Our proposed methodology was assessed using ROC curve performance matrices and accuracy score [31]. The accuracy score is a measure of the correctness of the model’s predictions. It quantifies the percentage of correct predictions made by the model out of the total predictions made. The following formula is used to determine the accuracy score:

$$Accuracy\ score = \frac{Number\ of\ Correct\ Predictions}{Total\ Number\ of\ Predictions} \times 100\% \quad (1)$$

A graphical representation known as the Receiver Operating Characteristic (ROC) curve is used to assess how well a binary classification model performs across various thresholds. For different threshold settings, it plots the actual positive rate (sensitivity) against the false positive rate (specificity). Specifically, lower values on the plot’s x-axis indicate lower false positives and higher true negatives, whereas higher values on the figure’s y-axis indicate higher true positives and lower false negatives. The area under the ROC curve (AUC-ROC) is commonly used as a summary metric to evaluate the overall performance of the classifier, with values ranging from 0 to 1. A higher AUC-ROC indicates better discrimination capacity of the model.

2.9 Validation of biomarkers gene expression

Using GEPIA2 (Gene Expression Profiling Interactive Analysis, <http://gepia2.cancer-pku.cn/>), a database of information obtained from the UCSC Xena server that contains 9736 tumour samples and 8587 normal samples, the expression levels of biomarkers in GBC and normal cases were confirmed. P-values less than 0.05 denoted statistically significant variations [32].

3 Results

3.1 DEG Identification

Initially from the GSE139682 and GSE100363 datasets, respectively, a total of 22829 and 22031 DEGs were discovered. Following execution of the revised P value requirement and minimal \log_2FC , 1800, 432 DEGs are found in accordance (Table 2). In the end, the common differential expression analysis between the tissues from gallbladder tumours and normal tissues produced 146 common differentially expressed genes among which the expression of 39 genes was found to be significantly up-regulated and 107 genes were down-regulated in GSE100363 and GSE139682 (Figure: 3). The volcano plot of different expression were shown in (Figure:4).

Accession Number	Before \log_2FC and adjusted p value filtration	After \log_2FC and adjusted p value filtration		
	Total DEGS	Total DEGS	Upregulated DEGS	Downregulated DEGS
GSE139682	22829	1800	759	1041
GSE100363	22031	432	191	241
Overlapped	20952	146	39	107

Table 2: Dataset analysis details before filtration and after \log_2FC and adjusted p value filtration.

Category	GO ID	%	P value
BP	Epidermis Development	7.692308	0.006651
BP	Keratinization	7.692308	0.007428
BP	Endodermal Cell Differentiation	5.128205	0.043789
BP	Cell Adhesion	10.25641	0.046459
BP	Establishment of Skin Barrier	5.128205	0.04655
BP	Intermediate Filament Organization	5.128205	0.093636
CC	Ciliary Membrane	5.128205	0.085086
CC	Cornified Envelope	5.128205	0.08375
CC	Intermediate Filament Cytoskeleton	5.128205	0.082411
CC	Integral Component of Membrane	33.33333	0.068537
CC	Hippocampal Mossy Fiber to CA3 Synapse	5.128205	0.060735
CC	Integral Component of Plasma Membrane	15.38462	0.054364
CC	Cytoskeleton	10.25641	0.044753
CC	Occluding Junction	5.128205	0.037162
CC	Apical Plasma Membrane	10.25641	0.019177
CC	Intermediate Filament	7.692308	0.017341
CC	Plasma Membrane	38.46154	0.011103
MF	Structural Molecule Activity	10.25641	0.003175
REACTOME	Signaling by Receptor Tyrosine Kinases	10.25641026	0.051975399
REACTOME	Formation of the Cornified Envelope	7.692307692	0.018876409
REACTOME	Keratinization	7.692307692	0.047712584
REACTOME	Extracellular Matrix Organization	7.692307692	0.085736649
REACTOME	Anchoring Fibril Formation	5.128205128	0.024375819
REACTOME	LDL Clearance	5.128205128	0.030780624
REACTOME	Laminin Interactions	5.128205128	0.048189704
REACTOME	Plasma Lipoprotein Clearance	5.128205128	0.059113989
REACTOME	Non-integrin Membrane-ECM Interactions	5.128205128	0.092681663
REACTOME	Assembly of Collagen Fibrils and other Multimeric Structures	5.128205128	0.095676523

Table 3: Gene Ontology analysis of upregulated DEGs using DAVID web tool.

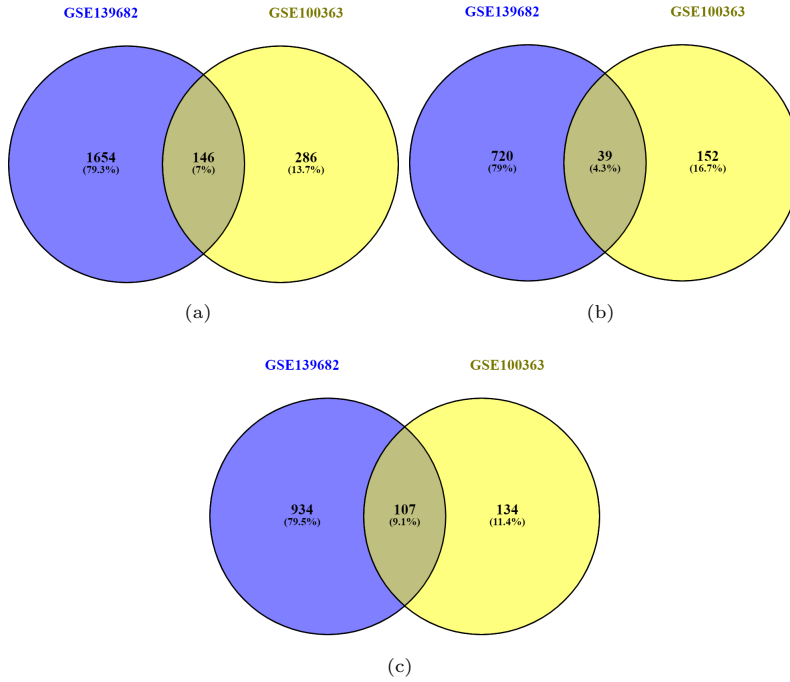


Fig. 3: Venn intersection diagrams of the DEGs of the two datasets: (a) represents the common DEGs, and (b) represents the common upregulated genes.(c) represents the common downregulated genes.

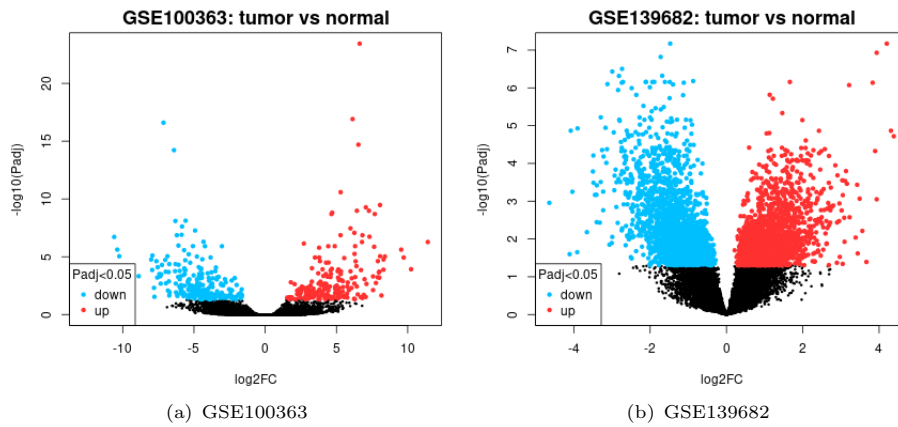


Fig. 4: Volcano plots of differentially expressed genes. Blue data points indicates down-regulated genes and red data points indicates up-regulated genes. The $|logFC| > 1$ for overexpression and $|logFC| < -1$ for downexpression was applied to set up differences. Black dots indicated genes that were not differentially expressed.

Category	GO ID	%	P value
BP	Cell Differentiation	12.38095	1.10E-04
BP	Nervous System Development	10.47619	3.16E-05
BP	Cell Adhesion	8.571429	0.005604
BP	Cell-Cell Adhesion	6.666667	3.51E-04
BP	Extracellular Matrix Organization	5.714286	0.002013
CC	Plasma Membrane	40.95238	1.40E-04
CC	Integral Component of Membrane	37.14286	0.003353
CC	Integral Component of Plasma Membrane	19.04762	3.49E-05
CC	Extracellular Space	19.04762	0.001877
CC	Extracellular Region	17.14286	0.02544
CC	Cell Surface	10.47619	0.001011
CC	Axon	8.571429	2.99E-04
CC	Dendrite	7.619048	0.005228
CC	External Side of Plasma Membrane	7.619048	0.00729
MF	Calcium ION Binding	8.571429	0.027692
MF	Heparin Binding	7.619048	2.39E-05
MF	Actin Binding	4.761905	0.081892
MF	Structural Molecule Activity	3.809524	0.066818
MF	Carbohydrate Binding	3.809524	0.073484
MF	Signaling Receptor Activity	3.809524	0.094202
REACTOME	Extracellular Matrix Organization	8.571429	1.14E-04
REACTOME	Collagen Biosynthesis and Modifying enzymes	3.809524	0.004569
REACTOME	Cell Surface Interactions at the Vascular Wall	4.761905	0.004872
REACTOME	Collagen Formation	3.809524	0.010334
REACTOME	Muscle Contraction	4.761905	0.019309
REACTOME	NGF-independant TRKA Activation	1.904762	0.024852
REACTOME	Cardiac Conduction	3.809524	0.028455
REACTOME	Activation of TRKA Receptors	1.904762	0.029749
REACTOME	Degradation of the Extracellular Matrix	3.809524	0.03306
REACTOME	Ligand-receptor Interactions	1.904762	0.039471
REACTOME	Neuronal System	5.714286	0.054045
REACTOME	Integrin Cell Surface Interactions	2.857143	0.067809
REACTOME	Signal Transduction	18.09524	0.079522
REACTOME	Activation of SMO	1.904762	0.086664
REACTOME	Hemostasis	6.666667	0.089655
REACTOME	Scavenging by Class A Receptors	1.904762	0.091256

Table 4: Gene Ontolgy analysis of downregulated DEGs using DAVID web tool.

3.2 Gene Ontology and Pathway Enrichment Analysis of DEGs

Using the DAVID online tool, GO functional and pathway enrichment analyses were carried out on the 146 common DEGs. To learn more about the function of the DEGs that were found, functional analysis was used. Significantly enriched GO terms and pathways of the discovered DEGs are revealed by the functional analysis. Based on the GO study, it can be inferred that the overexpressed DEGs are primarily linked to biological processes such as "Cell adhesion", "Epidermis development", and "Keratinization"; cellular components such as the "plasma membrane" and "integral membrane"; and molecular functions such as "structural molecule activity" (Table 3). Likewise, the investigation reveals that the downexpressed DEGs are primarily linked to "cell differentiation", "nervous system development", "cell adhesion" for biological process, "the plasma membrane", "integral component of membrane" for cellular component, "calcium ion binding", and "heparin binding" for molecular function. (Table 4). To further explore the pathways that were found to be enriched in DEGs, we performed a REACTOME pathway enrichment analysis next. The REACTOME pathway analysis revealed that the pathways involved in overexpression of DEGs were primarily enriched in "Signalling by Receptor Tyrosine Kinases" , "Formation

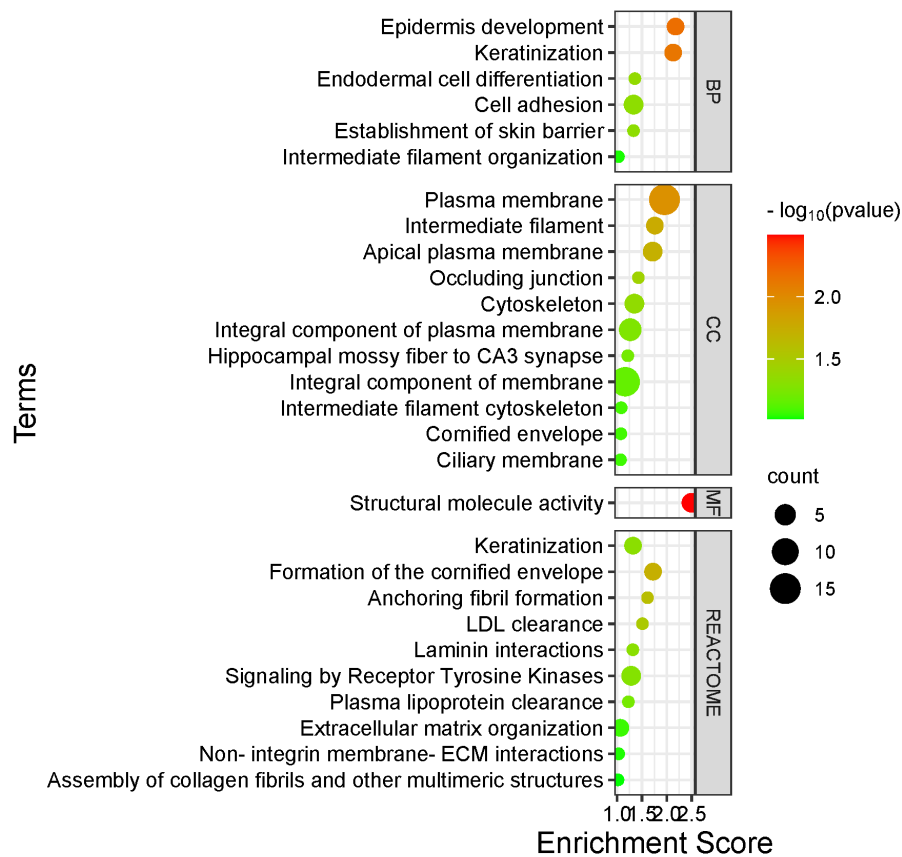


Fig. 5: Functional enrichment analyses: GO terms and REACTOME pathways for upregulated DEGs in this study. **BP:** Upregulated DEGs enriched in biological Process. **CC:** Upregulated DEGs enriched in cellular component. **MF:** Upregulated DEGs enriched in molecular function. The size of the bubble indicates the enrichment score; colors indicate enrichment significance.

of the Cornified Envelope” , ”Keratinization” , and ”Extracellular Matrix Organisation” pathway (Table 3). Furthermore, ”Signal Transduction” , ”Extracellular Matrix Organisation” , and ”Hemostasis” pathways were the key ones where downexpressed DEGs were enriched (Table 4). Using an enrichment dot bubble diagram made with the bioinformatics website and GO-enriched BP/MF/CC and REACTOME, the GO keywords and pathways for both overexpressed DEGs (Figure 5) and downexpressed DEGs (Figure 6) were visualised.

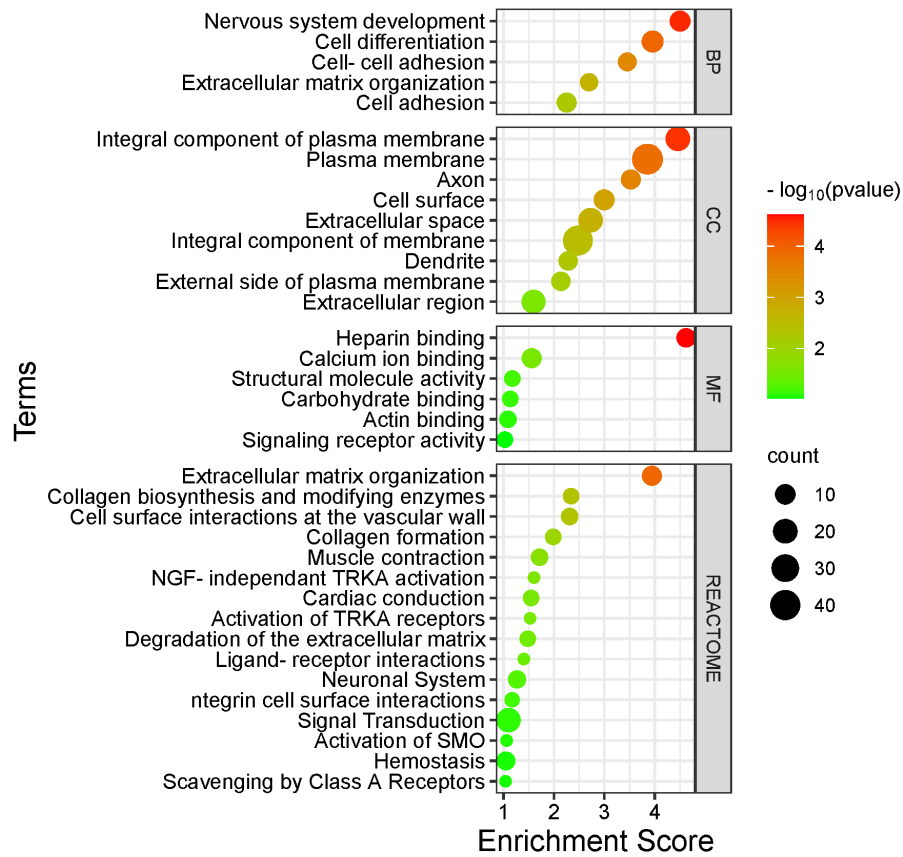


Fig. 6: Functional enrichment analyses: GO terms for downregulated differentially expressed genes (DEGs) in this study and REACTOME pathways for DEGs. The size of the bubble indicates the enrichment score; colors indicate enrichment significance

3.3 PPI Construction and Screening for Hub Genes

Utilising Cytoscape and the STRING online database, we constructed a DEG PPI network to investigate the protein networks linked to identified genes (Figure 7). Next, employing the cytoHubba plugin, the PPI network was loaded into the Cytoscape software to visualise and identify the hub genes. We subsequently acquired the top-15 hub genes for each of the three topological ranking algorithms: Closeness Centrality, Maximum Neighbourhood Component (MNC), and Degree (Figure 8). Amazingly, we discovered that just 11 of the hub genes were identified by all three ranking methods (Figure 8, Table 5). The 11 "real" hub genes were found at the intersection of the hub genes produced by the three methods.

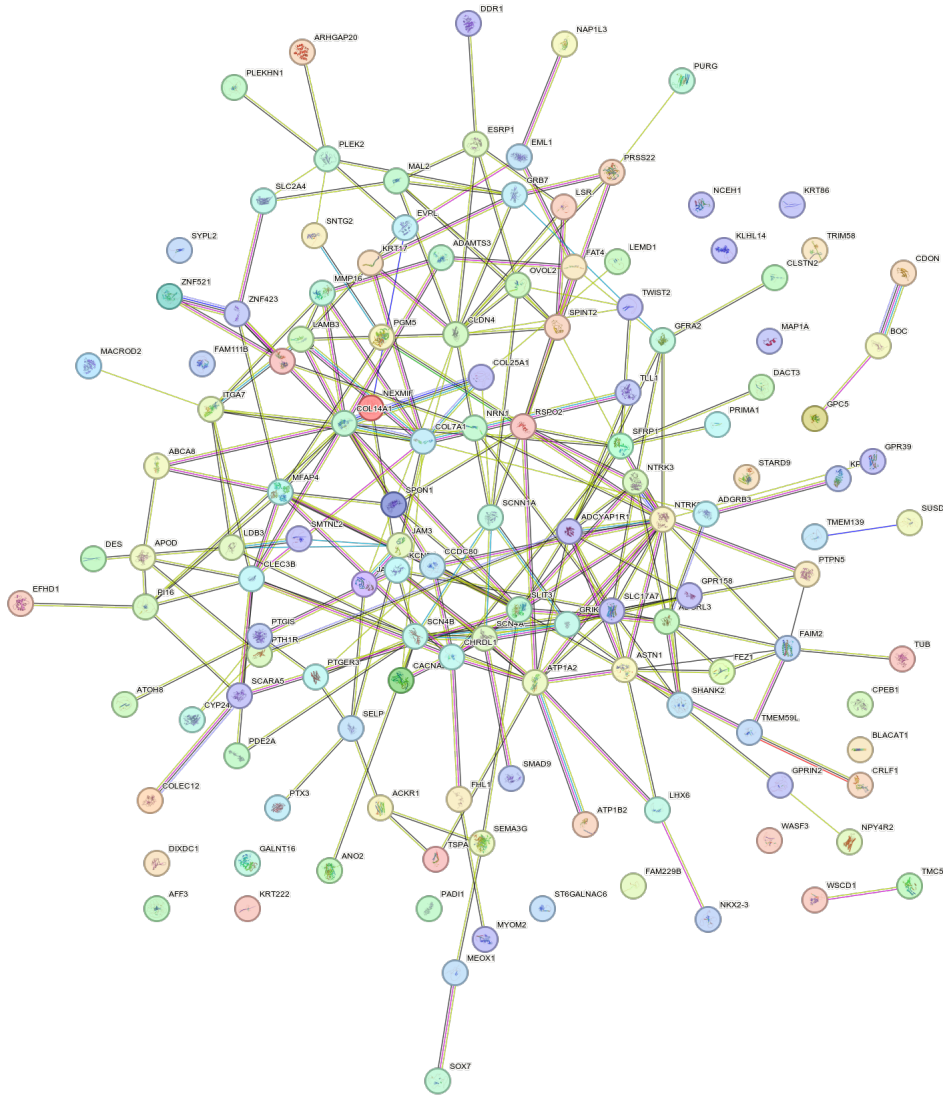


Fig. 7: PPI network of 146 promising target genes in gall bladder cancer based on the string website.

3.4 Identification of significant genes using feature selection methods

By employing feature selection techniques to identify the gene sets that most effectively contribute to the prediction job, we also ascertained the features required to construct the ML models. The 147 DEGs were used in the application of the recursive feature elimination and pearson correlation feature selection procedures. To choose the most

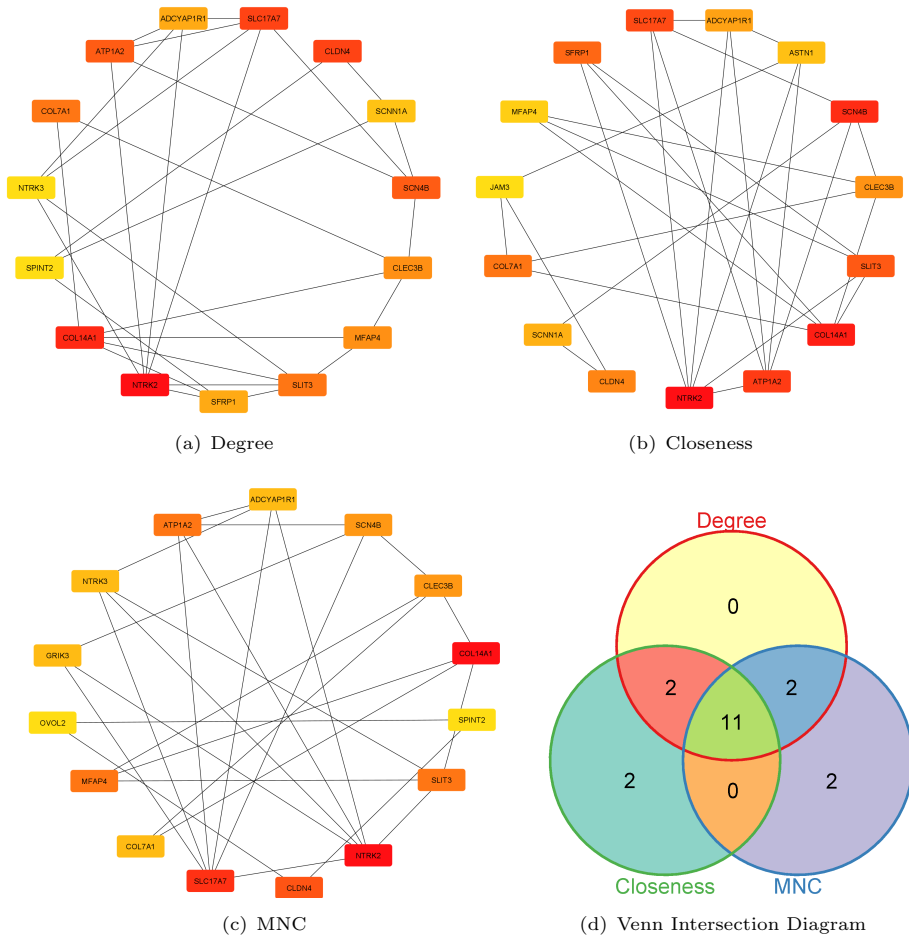


Fig. 8: (a-c) Hub genes identification with the CytoHubba plugin in Cytoscape software. Three different metrics were used: DEGREE, MNC, closeness. (d) A Venn diagram used to identify 11 hub genes in gall bladder cancer.

suitable group of features for both approaches, we experimented with a number of threshold values. Through defining the correlation scores above 0.9, we succeeded to get gene groups of 20 using Pearson correlation method. Furthermore, by setting the *n_features_to_select* to 20 and utilising the SVM approach as an *estimator*, we succeeded to get gene groups of 20 through the use of the recursive feature elimination method. Table 5 lists the significant genes that have been identified using both feature selection methods.

Methods	Identified Genes
11 "real" hub genes identified at intersection of hub genes produced by three ranking algorithms.	NTRK2, COL14A1, SCN4B, ATP1A2, SLC17A7, SLIT3, COL7A1, CLDN4, CLEC3B, ADCYAP1R1, MFAP4
Significant genes identified through the Pearson Correlation FSM.	ABCA8, ADAMTS3, AFAP1-AS1, AFF3, ASTN1, CCAT1,CLDN4,COL7A1,CYP24A1, DDR1, ESRP1, EVPL, FAM111B, GALNT16, KCNAB1, PTGIS, TMEM59L, RAMP2 - AS1, SCARNA5, SLC22A4, PTX3
Significant genes identified through Recursive Feature Elimination FSM	ATP1B2, CLDN4, COLEC12,CRLF1,DDR1, EFHD1, FAM111B, FHL1, GALNT16, JAM3, LSR, NCEH1, NRN1,PTGIS,SFRP1,SPINT2,SPON1,TSPAN7,TUB, ST6GALNAC6

Table 5: Identification of real hub genes by PPI network and significant genes by feature selection methods.

3.5 Evaluating the prediction performance of ML models on independent dataset

We assessed the variations in the prediction abilities of the two machine learning models, RF and SVM, on independent dataset(GSE139682) upon feeding them distinct feature sets of 11 'real' hub genes and of genes determined by the two feature selection techniques independently. Hence, we created three separate datasets for each biomarker identification methods. First dataset contains the 11 real hub genes as features; second and third dataset contains genes identified by pearson correlation and recursive feature elimination method respectively as features. Following that, these datasets were classified, and the classification abilities of individual feature selection techniques and classification algorithms were examined. The accuracy score of these investigations during the evaluation procedure are shown in table 6 and in figure 9. Figure 10 shows the AUROC curve of the independent testing dataset for SVM, RF classifiers with the highest performance for the identified different gene subsets. In all cases, the result shows that the subset of real hub genes outperformed than other genes subsets. On the other hand, the gene subset identified by Recursive Feature Elimination method provided worst performance. These findings imply that classifiers built using hub genes were able to attain good prediction performances.

Models	'Real' hub genes	Significant Genes Identified by feature selection methods	
		Pearson Correlation Method	Recursive Feature Elimination Method
SVM	0.85	0.9	0.75
RF	0.9	0.75	0.7

Table 6: The accuracy scores of Support vector machine and Random Forest classification model based on real hub genes identified at the intersection of three hub gene ranking algorithm and genes identified by Pearson Correlation Method and Recursive Feature Elimination Method

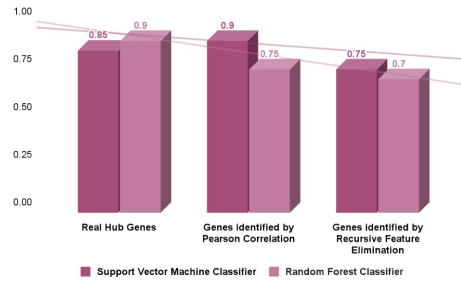


Fig. 9: The graphical representation of accuracy scores of Support vector machine and Random Forest classification model based on real hub genes identified at the intersection of three hub gene ranking algorithm and genes identified by Pearson Correlation Method and Recursive Feature Elimination Method

3.6 Validation of hub gene expression

Hub gene expression was confirmed using the GEPIA database, with a P -value < 0.05 and a $Log_2FC > 1$ criterion. GEPIA box plots showed that all hub gene expressions in GBC patients were considerably upregulated in the SLIT3, COL7A1, CLDN4 (Figure: 11). There are little statistical difference in other genes.

4 Discussion

Gallbladder cancer (GBC) is the most common cause of disease among biliary tract neoplasms, comprising 80% - 95% [33]. Based to GLOBOCAN's (Global Cancer Observatory) 2020 cancer data [34], GBC was the 24th most common cause of cancer worldwide in 2020, with over 115,949 newly reported cases. The amount of patients with a GBC diagnosis reached at nearly 84,695 that year because of the severe form of the cancer. The overall global incidence has been rising over recent years, despite regional variations in incidence rates. This trend is expected to continue as risk factors grow more common among populations [35]. The goal and challenge for medical and scientific research has always been to identify the molecular mechanism and biomarkers associated with the onset and progression of gallbladder cancer. This research has significant research value in enhancing the diagnosis, efficacy of treatment, and prognosis survival of lung cancer patients.

The current work aims to comprehensively identify potential genes and pathways associated with gallbladder cancer by bioinformatics analysis and machine learning methods. From the Gene Expression Omnibus database, gene expression data (expression profiles GSE100363 and GSE139682) were acquired. Afterward, a total of 432 and 1800 potential DEGs were obtained from two different datasets. Of these, 146 were identified as common potential DEGs, with 39 of them being up-regulated genes and 107 being down-regulated genes related to gallbladder cancer. Next, in order to explore up-regulated and down-regulated genes, we carried out enrichment studies of GO analysis (three methods: CC, MF, and BP), pathway analysis using REACTOM database.

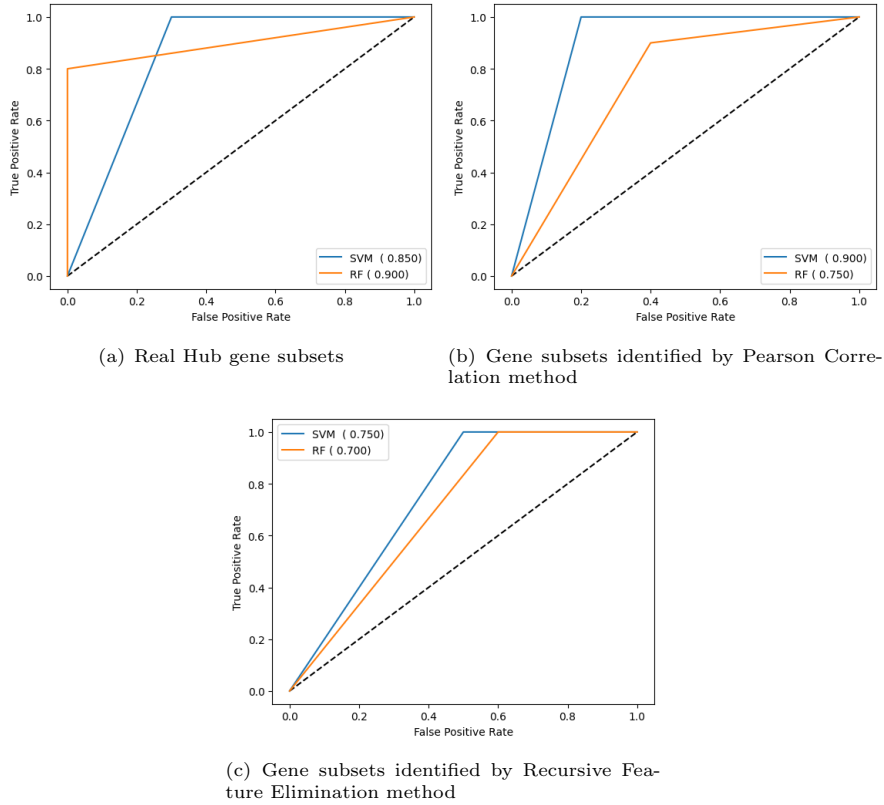


Fig. 10: The ROC curves of Support vector machine and Random Forest classification model based on real hub genes identified at the intersection of three hub gene ranking algorithm and genes identified by Pearson Correlation Method and Recursive Feature Elimination Method

According to the GO and REACTOME study, the overexpressed DEGs are mainly associated with biological processes like "cell adhesion," "epidermis development," and "keratinization," cellular components like "integral membrane" and "plasma membrane," molecular functions like "structural molecule activity" and pathways like "Signalling by Receptor Tyrosine Kinase. Likewise, the investigation reveals that the downexpressed DEGs are primarily linked to "cell differentiation", "nervous system development", "cell adhesion" for biological process, "the plasma membrane", "integral component of membrane" for cellular component, "calcium ion binding", and "heparin binding" for molecular function and "Signal Transduction" for pathways.

In order to evaluate the interactional links, we also built a PPI network. After that, we obtained the top-15 hub genes for each of the three ranking algorithms: Closeness Centrality, MNC, and Degree. Surprisingly, we found that just 11 of the hub genes—which were regarded as "real" hub genes—were recognised by all three ranking techniques. Additionally, SLIT3, COL7A1, and CLDN4 hub gene expressions in GBC

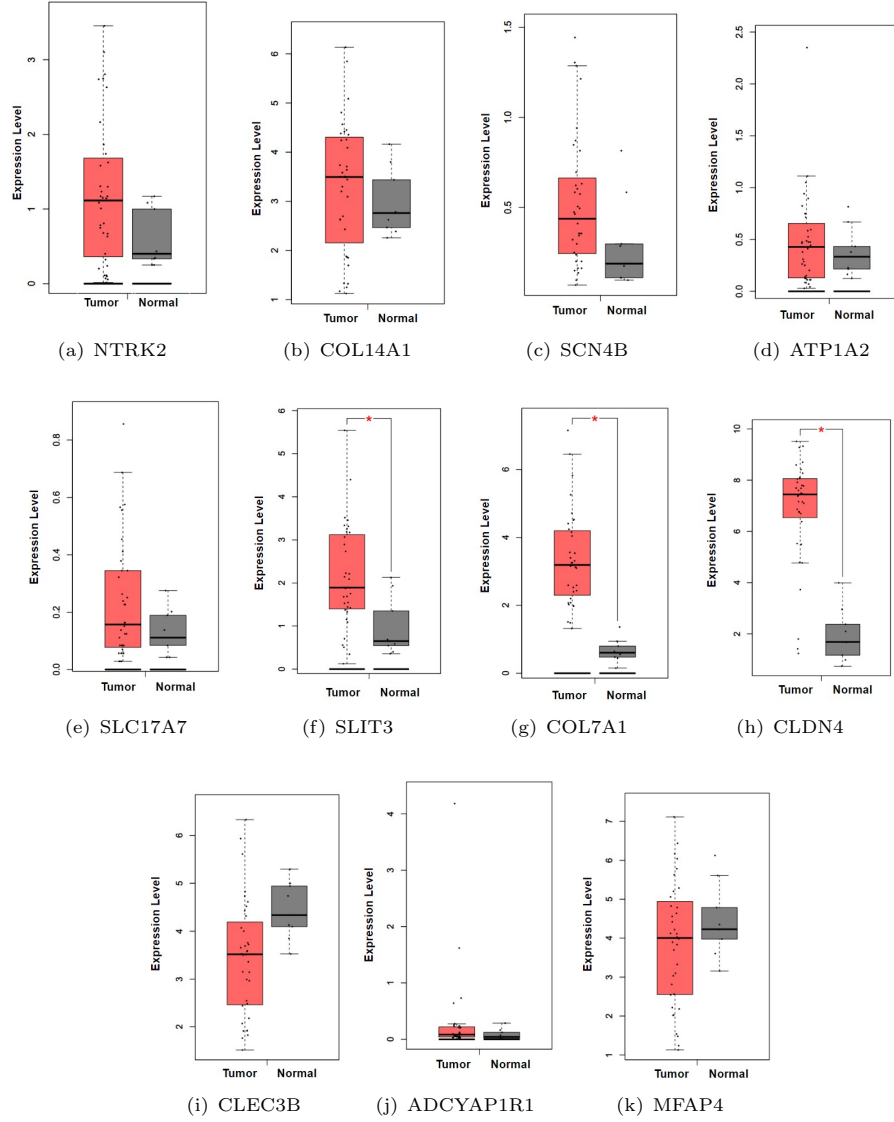


Fig. 11: Validation of hub gene expression: GEPIA files are used to create boxplots that display the hub gene expression in GBC patients and healthy controls.

patients were significantly elevated, according to GEPIA box plots. Other genes show minimal statistical differences.

Additionally, in this investigation, we employed feature selection methods including Recursive Feature Elimination (RFE) and Pearson Correlation to identify the significant DEGs that most effectively separate unhealthy samples from the healthy controls. Then, using the SVM and RF algorithms, the genuine hub genes and significant genes

that were found using the feature selection method were trained on the GSE 100363 dataset to create a machine learning model. In order to validate the biomarkers, the model was lastly validated using the independent GSE 139682 dataset. Nonetheless, the outcomes showed that the subset of real hub genes outperformed the others, suggesting that these candidate genes could be used as potential biomarkers for GBC diagnosis.

5 Conclusions

In this study, we analyzed gene expression data using bioinformatics and machine learning approach, which may supplement traditional clinical prognostic factors, enabling clinicians to provide more effective therapeutic intervention and personalized treatment for gall bladder cancer. Here, We designed a computational method that exploits multiple hub gene ranking methods and feature selection methods with machine learning and bioinformatics to identify biomarkers. In this study, We have identified 11 key genes with diagnostic and prognostic values in GBC. We identified these genes by using comprehensive bioinformatics and machine learning technology.

References

- [1] Hundal, R., Shaffer, E.A.: Gallbladder cancer: epidemiology and outcome. *Clinical epidemiology*, 99–109 (2014)
- [2] Rakić, M., Patrlj, L., Kopljar, M., Kliček, R., Kolovrat, M., Loncar, B., Basic, Z.: Gallbladder cancer. *Hepatobiliary surgery and nutrition* **3**(5), 221 (2014)
- [3] Siegel, R.L., Miller, K.D., Fuchs, H.E., Jemal, A., *et al.*: Cancer statistics, 2021. *Ca Cancer J Clin* **71**(1), 7–33 (2021)
- [4] Valle, J.W., Kelley, R.K., Nervi, B., Oh, D.-Y., Zhu, A.X.: Biliary tract cancer. *The Lancet* **397**(10272), 428–444 (2021)
- [5] Gourgiotis, S., Kocher, H.M., Solaini, L., Yarollahi, A., Tsiambas, E., Salemis, N.S.: Gallbladder cancer. *The American Journal of Surgery* **196**(2), 252–264 (2008)
- [6] Chun, Y.S., Pawlik, T.M., Vauthey, J.-N.: of the ajcc cancer staging manual: pancreas and hepatobiliary cancers. *Annals of surgical oncology* **25**, 845–847 (2018)
- [7] Mantripragada, K.C., Hamid, F., Shafqat, H., Olszewski, A.J.: Adjuvant therapy for resected gallbladder cancer: analysis of the national cancer data base. *Journal of the National Cancer Institute* **109**(2), 202 (2017)
- [8] Chen, M., Cao, J., Bai, Y., Tong, C., Lin, J., Jindal, V., Barchi, L.C., Nadalin, S., Yang, S.X., Pesce, A., *et al.*: Development and validation of a nomogram

for early detection of malignant gallbladder lesions. *Clinical and translational gastroenterology* **10**(10) (2019)

- [9] Tauriello, D.V., Palomo-Ponce, S., Stork, D., Berenguer-Llargo, A., Badia-Ramentol, J., Iglesias, M., Sevillano, M., Ibiza, S., Cañellas, A., Hernando-Momblona, X., *et al.*: Tgf β drives immune evasion in genetically reconstituted colon cancer metastasis. *Nature* **554**(7693), 538–543 (2018)
- [10] Wu, M.-J., Chen, Y.-S., Kim, M.R., Chang, C.-C., Gampala, S., Zhang, Y., Wang, Y., Chang, C.-Y., Yang, J.-Y., Chang, C.-J.: Epithelial-mesenchymal transition directs stem cell polarity via regulation of mitofusin. *Cell metabolism* **29**(4), 993–1002 (2019)
- [11] Zheng, L., Xu, M., Xu, J., Wu, K., Fang, Q., Liang, Y., Zhou, S., Cen, D., Ji, L., Han, W., *et al.*: Elf3 promotes epithelial–mesenchymal transition by protecting zeb1 from mir-141-3p-mediated silencing in hepatocellular carcinoma. *Cell death & disease* **9**(3), 387 (2018)
- [12] Civenni, G., Bosotti, R., Timpanaro, A., Vazquez, R., Merulla, J., Pandit, S., Rossi, S., Albino, D., Allegrini, S., Mitra, A., *et al.*: Epigenetic control of mitochondrial fission enables self-renewal of stem-like tumor cells in human prostate cancer. *Cell metabolism* **30**(2), 303–318 (2019)
- [13] Raphael, B.J., Hruban, R.H., Aguirre, A.J., Moffitt, R.A., Yeh, J.J., Stewart, C., Robertson, A.G., Cherniack, A.D., Gupta, M., Getz, G., *et al.*: Integrated genomic characterization of pancreatic ductal adenocarcinoma. *Cancer cell* **32**(2), 185–203 (2017)
- [14] Kinde, I., Bettgowda, C., Wang, Y., Wu, J., Agrawal, N., Shih, I.-M., Kurman, R., Dao, F., Levine, D.A., Giuntoli, R., *et al.*: Evaluation of dna from the papanicolaou test to detect ovarian and endometrial cancers. *Science translational medicine* **5**(167), 167–41674 (2013)
- [15] Kulasingam, V., Diamandis, E.P.: Strategies for discovering novel cancer biomarkers through utilization of emerging technologies. *Nature clinical practice Oncology* **5**(10), 588–599 (2008)
- [16] Auslander, N., Gussow, A.B., Koonin, E.V.: Incorporating machine learning into established bioinformatics frameworks. *International journal of molecular sciences* **22**(6), 2903 (2021)
- [17] Barrett, T., Wilhite, S.E., Ledoux, P., Evangelista, C., Kim, I.F., Tomashevsky, M., Marshall, K.A., Phillippy, K.H., Sherman, P.M., Holko, M., *et al.*: Ncbi geo: archive for functional genomics data sets—update. *Nucleic acids research* **41**(D1), 991–995 (2012)
- [18] Kong, X., Wang, C., Wu, Q., Wang, Z., Han, Y., Teng, J., Qi, X.: Screening

- and identification of key biomarkers of depression using bioinformatics. *Scientific Reports* **13**(1), 4180 (2023)
- [19] Xu, Z., Zhou, Y., Cao, Y., Dinh, T.L.A., Wan, J., Zhao, M.: Identification of candidate biomarkers and analysis of prognostic values in ovarian cancer by integrated bioinformatics analysis. *Medical oncology* **33**, 1–8 (2016)
- [20] Oliveros, J.C.: Venny. an interactive tool for comparing lists with venn diagrams. <http://bioinfogp.cnb.csic.es/tools/venny/index.html> (2007)
- [21] Reimand, J., Isserlin, R., Voisin, V., Kucera, M., Tannus-Lopes, C., Rostamianfar, A., Wadi, L., Meyer, M., Wong, J., Xu, C., *et al.*: Pathway enrichment analysis and visualization of omics data using g: Profiler, gsea, cytoscape and enrichmentmap. *Nature protocols* **14**(2), 482–517 (2019)
- [22] Ashburner, M., Ball, C.A., Blake, J.A., Botstein, D., Butler, H., Cherry, J.M., Davis, A.P., Dolinski, K., Dwight, S.S., Eppig, J.T., *et al.*: Gene ontology: tool for the unification of biology. *Nature genetics* **25**(1), 25–29 (2000)
- [23] Croft, D., O’kelly, G., Wu, G., Haw, R., Gillespie, M., Matthews, L., Caudy, M., Garapati, P., Gopinath, G., Jassal, B., *et al.*: Reactome: a database of reactions, pathways and biological processes. *Nucleic acids research* **39**(suppl.1), 691–697 (2010)
- [24] Huang, D.W., Sherman, B.T., Tan, Q., Collins, J.R., Alvord, W.G., Roayaei, J., Stephens, R., Baseler, M.W., Lane, H.C., Lempicki, R.A.: The david gene functional classification tool: a novel biological module-centric algorithm to functionally analyze large gene lists. *Genome biology* **8**(9), 1–16 (2007)
- [25] Franceschini, A., Szklarczyk, D., Frankild, S., Kuhn, M., Simonovic, M., Roth, A., Lin, J., Minguez, P., Bork, P., Von Mering, C., *et al.*: String v9. 1: protein-protein interaction networks, with increased coverage and integration. *Nucleic acids research* **41**(D1), 808–815 (2012)
- [26] Smoot, M.E., Ono, K., Ruscheinski, J., Wang, P.-L., Ideker, T.: Cytoscape 2.8: new features for data integration and network visualization. *Bioinformatics* **27**(3), 431–432 (2011)
- [27] Kohl, M., Wiese, S., Warscheid, B.: Cytoscape: software for visualization and analysis of biological networks. *Data mining in proteomics: from standards to applications*, 291–303 (2011)
- [28] Chin, C.-H., Chen, S.-H., Wu, H.-H., Ho, C.-W., Ko, M.-T., Lin, C.-Y.: cytohubba: identifying hub objects and sub-networks from complex interactome. *BMC systems biology* **8**(4), 1–7 (2014)
- [29] Breiman, L.: Random forests. *Machine learning* **45**, 5–32 (2001)

- [30] Khatun, R., Akter, M., Islam, M.M., Uddin, M.A., Talukder, M.A., Kamruzaman, J., Azad, A., Paul, B.K., Almoyad, M.A.A., Aryal, S., *et al.*: Cancer classification utilizing voting classifier with ensemble feature selection method and transcriptomic data. *Genes* **14**(9), 1802 (2023)
- [31] Fakoor, R., Ladhak, F., Nazi, A., Huber, M.: Using deep learning to enhance cancer diagnosis and classification. In: *Proceedings of the International Conference on Machine Learning*, vol. 28, pp. 3937–3949 (2013). ACM New York, NY, USA
- [32] Tang, Z., Li, C., Kang, B., Gao, G., Li, C., Zhang, Z.: Gepia: a web server for cancer and normal gene expression profiling and interactive analyses. *Nucleic acids research* **45**(W1), 98–102 (2017)
- [33] Huang, J., Patel, H.K., Boakye, D., Chandrasekar, V.T., Koulaouzidis, A., Lucero-Prisno III, D.E., Ngai, C.H., Pun, C.N., Bai, Y., Lok, V., *et al.*: Worldwide distribution, associated factors, and trends of gallbladder cancer: a global country-level analysis. *Cancer letters* **521**, 238–251 (2021)
- [34] Khandelwal, A., Malhotra, A., Jain, M., Vasquez, K.M., Jain, A.: The emerging role of long non-coding rna in gallbladder cancer pathogenesis. *Biochimie* **132**, 152–160 (2017)
- [35] Liu, Y., Ding, W., Yu, W., Zhang, Y., Ao, X., Wang, J.: Long non-coding rnas: Biogenesis, functions, and clinical significance in gastric cancer. *Molecular Therapy-Oncolytics* **23**, 458–476 (2021)